JOM, Vol. 67, No. 3, 2015
DOI: 10.1007/s11837-015-1303-1

Compact Process for the Preparation of Microfine Spherical High-Niobium-Containing TiAl Alloy Powders

J.B. TONG,[1] X. LU,[1,2,3] C.C. LIU,[1] L.N. WANG,[1,2] and X.H. QU[1,2,4]

1.—School of Materials Science and Engineering, University of Science and Technology Beijing, Beijing 100083, People's Republic of China. 2.—Institute for Advanced Materials and Technology, University of Science and Technology Beijing, Beijing 100083, People's Republic of China. 3.—e-mail: luxin@ustb.edu.cn. 4.—e-mail: quxh@ustb.edu.cn

High-Nb-containing TiAl alloys are a new generation of materials for high-temperature structural applications because of their superior high-temperature mechanical properties. The alloy powders can be widely used for additive manufacturing, thermal spraying, and powder metallurgy. Because of the difficulty of making microfine spherical alloy powders in quantity by conventional techniques, a compact method was proposed, which consisted of two-step ball milling of elemental powders and subsequent radio frequency (RF) argon plasma spheroidization. In comparison with conventional mechanical alloying techniques, the two-step milling process can be used to prepare alloy powders with uniform scale in a short milling time with no addition of process control agent. This makes the process effective and less contaminating. After RF argon plasma spheroidization, the powders produced exhibit good sphericity, and the number-average diameter is about 8.2 μm with a symmetric unimodal particle size distribution. The powders perform high composition homogeneity and contain predominately supersaturated α_2-Ti_3Al phase. The oxygen and carbon contents of the spheroidized powder are 0.47% and 0.050%, respectively.

INTRODUCTION

Nowadays, structural materials with outstanding high-temperature mechanical properties are demanded with the rapid development in the aerospace, automobile and construction fields. Because of relatively low specific strength, traditional Fe, Ni, Co-based high-temperature alloys can hardly satisfy the novel application requirements. TiAl intermetallic compounds have attracted much attention for their outstanding strength and creep resistance at elevated temperature as well as their low density. To further improve the performance of TiAl alloys, the influences of introducing other elements on the properties have been investigated.[1–3] Previous studies have demonstrated that, with Nb addition, the high-temperature strength and oxidation resistance of the γ-TiAl intermetallics were greatly improved while the low density was maintained.[4,5] Consequently, high-Nb-containing TiAl alloys are considered as the next generation of materials for high-temperature structural applications.[6–8] On the other hand, the applications of high-Nb-containing TiAl alloys are still limited because of their low ductility and plasticity at ambient temperature, which may bring about the difficulties in processing and machining. To solve this problem, novel techniques need to be developed for the fabrication of TiAl alloys. Additive manufacturing (three-dimensional printing) is one such technology. Compared with traditional processes, additive manufacturing in a layer-by-layer way can extend the design freedom of parts in terms of applications. Considerable recognition has been gained of additive manufacturing since it was introduced, and it is regarded as a revolutionary process for the manufacturing industry.[9–11]

Fabrication Technologies of TiAl-Based Alloy Powders

In recent years, with the development of three-dimensional metal printing, more demanding re-

(Published online February 10, 2015)

quirements have been raised for powder materials.[12,13] Especially for the fabrication of TiAl-based alloy parts by additive manufacturing, the preparation of alloy powders with high quality is of prime importance. In addition, qualified alloy powders are also in great need in many other current technology fields such as powder metallurgy, rapid prototyping, and thermal spraying coating.[14,15] As a consequence, there is a need to continuously develop and improve the preparation techniques for the production of TiAl alloy powders with microfine size, good flowability, uniform microstructure, high purity, and low cost.

Several conventional powder preparation methods, including inert gas atomization, rotating electrode atomization, mechanical alloying (MA), and self-propagating high-temperature syntheses (SHS), have been employed to fabricate the TiAl-based alloy powders.

Traditional inert gas atomization has been widely used to produce spherical TiAl alloy powders with good compositional homogeneity. However, reactive metals can be easily contaminated by introducing O, N, and other impurity elements from the crucible used. Moreover, the powders thus produced possess a relatively large particle size. According to Gerling et al., the produced TiAl alloy powders exhibit a particle size range of 32–355 μm.[16] By means of plasma rotate electrode pulverization and electrode induction melting gas atomization (EIGA), spherical TiAl powders can also be fabricated. Without the contamination from the crucible, the purity can be significantly improved. Similar to the traditional inert gas atomization technique, the powders produced are still coarse with only a small proportion of fine powders. Wegmann et al.[17] have successfully produced Ti-46at.%Al-9at.%Nb and Ti-48.9at.%Al alloy powders with EIGA. The powder particle ranges are 20–350 μm in diameter, and the proportion of particles smaller than 45 μm is less than 25%. Whereas fine powders can be easily prepared by the MA process from elemental powders, it is hard to acquire fully alloyed powders. Farhang et al.[18] have found that it is difficult for Ti-Al intermetallic phases to form even with milling time up to 100 h. In addition, prolonged milling may induce a certain amount of impurities not only from the milling balls and vials but also from the milling process control agent (PCA). SHS is an effective route for the preparation of microfine TiAl alloy powders in a short and simple process. However, when some alloying elements are introduced, such as Nb, the reaction and diffusion are often incomplete, leading to the composition inhomogeneity of powders. Forouzanmehr et al.[19] and Kumaran et al.[20] have prepared TiAl powders with a combination of MA and the SHS process. The amorphous powders formed by MA for 20-40 h are annealed at 700°C to 750°C and powders consisting of γ and α_2 phase are obtained. It is shown that fine TiAl alloy powders with homogenous composition can be produced with this method, but the impurity contents are high. In this regard, no current powder preparation techniques can meet the requirement of making microfine spherical TiAl alloy powders with composition uniformity and high purity. They all need to be optimized and improved to achieve the best efficiency and cost.

Plasma Spheroidization Technology

As an advanced powder surface processing method, radio frequency (RF) plasma technology is advantageous over conventional techniques, such as high heating temperature fields (~8000 K), extremely rapid quenching rates (~10^{-6} K/s), and low pollution.[21–23] It can effectively process powders with high purity, good sphericity, small particle size, and without inside pores. With alternating or direct current the blowing-in argon and other gas are ionized to form a plasma torch, which is made up of a great amount of electrons and ions. Flying through an extremely high-temperature plasma torch, powders with irregular shape are melted and form spherical droplets under surface tension. Then, these droplets are cooled and solidified rapidly to form spherical-shaped particles.

In previous studies, spherical powders of refractory metals[24,25] and ceramics[26,27] with high melting points have been produced by plasma spheroidization processing. In our previous work,[28] the method was used for the first time to spheroidize the

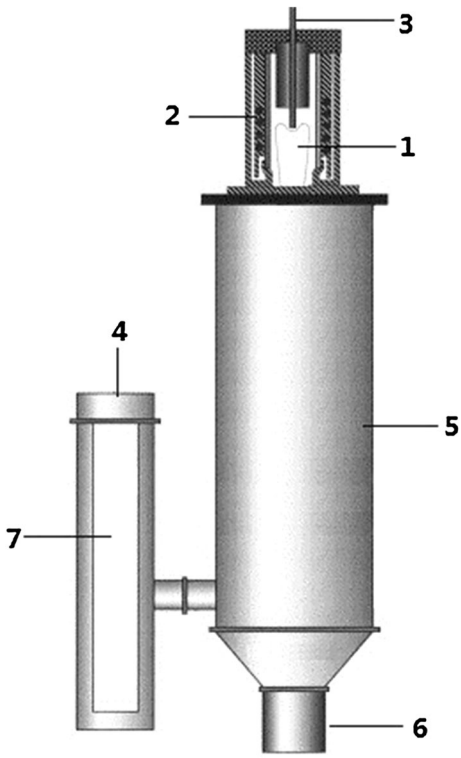

Fig. 1. Schematic of a powder spheroidization system. This system includes: 1—plasma torch, 2—induction coils, 3—powder feeder, 4—vacuum, 5—cooler, 6—collector, and 7—filter

irregular-shaped high-Nb-containing TiAl alloy powders crushed from ingot materials. It has proved the feasibility of making microfine spherical TiAl intermetallic powders by means of RF plasma technology.

In this research summary, we present our recent progress on a new route for making microfine spherical TiAl-Nb alloy powders from elemental materials. A compact and less contaminative two-step ball milling process followed by vacuum annealing was developed to synthesize and refine the TiAl-Nb alloy powders. Subsequently, the irregular-shaped alloy powders were processed using an RF plasma spheroidization system for spheroidization. The fabrication process and powder characterization were analyzed.

EXPERIMENTAL PROCEDURES

Ti, Al and Nb elemental powders with ~500 mesh and high purity (≥99.5%) were employed in the research. The raw powders were mixed in a blender for 6 h to obtain a nominal composition of Ti-45Al-8.5Nb (at.%). Initially, the powder mixture was milled for 4 h with a QM-1SP4 planetary ball milling machine. The milling process was carried out in a high-purity argon atmosphere with no addition of PCA. The rotation speed is 350 r/min, and the ball-to-powder weight ratio is 8:1. This standard milling procedure named as "primary milling" is to obtain composite particles with uniform and ultrafine chemical component, so that the diffusion distances among elements can be shortened. The powders obtained by primary milling were subsequently annealed from 1250°C to 1400°C for 2 h in vacuum (10^{-3} Pa) and then furnace cooled to room temperature. During the powder annealing, the alloying of Ti-Al-Nb occurred by reaction synthesis and diffusion. Then, the coarse alloy particles were refined by a secondary milling operation. The procedure was performed for 30 min in a vibration ball milling machine with the frequency of 1400 Hz. The milling is in argon atmosphere with a ball-to-powder ratio of 10:1. To avoid the overheating of milling cans, the mill was paused for 5 min after a 5 min run, and 2 wt.% alcohol was added to reduce the bonding between balls and powders.

Finally, the irregular microfine powders were processed by the RF plasma spheroidization system with the argon gas flow rate of 85 L/min, the input power of 45 KW, and the negative pressure of −1000 Pa. The system is schematically shown in Fig. 1.[29]

A Siemens D5000 x-ray diffraction (XRD) meter (SIMENS, Germany) using Cu radiation was used to analyze the phase constitution of the powders. The observation of microstructure morphology and the analysis of element distribution were performed by a LEO1450 scanning electron microscope (SEM) (ZEISS, Germany) equipped with KEVEX sigma energy-dispersive spectrometer (Kevex Inc., Newark, DE). The particle size distribution was examined by using an LMS-30 laser particle size analyzer (SEISHIN ENTERPRISE Co., Ltd., Tokyo, Japan). The impurity contents were measured by the high-frequency combustion-infrared absorption method and the inert gas impulse infrared thermal conductivity method.

The parameter of number-average diameter ($D(1,0)$) was introduced to characterize the powder size. From the detected particle size distribution data, the value of $D(1,0)$ can be calculated using Eq. 1, where d_i means detected particle diameter and n_i (%) indicates the percentage of the particles with the diameter of d_i (μm).

$$D(1,0) = \frac{\sum\left(n_i \cdot \sqrt{d_{i-1} \cdot d_i}\right)}{\sum n_i} \tag{1}$$

RESULTS AND DISCUSSION

Synthesis of High-Nb-Containing TiAl Alloy Powders

Figure 2 shows the surface and internal morphologies of powders obtained from primary milling. It is noted that powder particles significantly grow

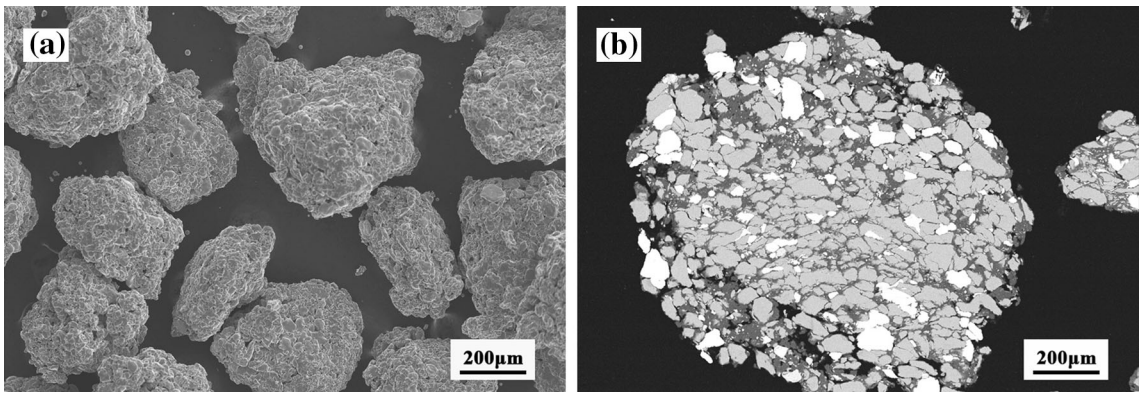

Fig. 2. Morphology of powder after primary milling: (a) SEM of surface and (b) BSE of profile.

up with the maximum particle diameter reaching about 200 μm. Backscattered electron (BSE) micrographs show that in each agglomerate, ultrafine Ti and Nb particles were embedded into the Al matrix. Due to the higher plasticity of Al than the other elements, severe plastic deformation occurs to Al particles with repeated grinding and rolling, forming a lamellate structure. The superficial area of Al particles has increased substantially. On the other hand, the Ti, Nb particles with high hardness tend to break into ultrafine particles, which are gradually embedded into soft Al particles, forming some composite particles. With the proceeding of milling, cold welding continuously happens among the composite particles, leading to an increased particle size. As a result, coarse particles, in which fine Nb and Ti components are evenly embedded into the Al matrix, can be produced.

The profile morphologies of annealed powders with different annealing temperatures are portrayed in Fig. 3. Generally, the microstructure tends to become homogenous with the increasing annealing temperature. The bright zones enriched with Nb can be observed in the powders annealed from 1250°C to 1350°C. The composition of the powders annealed at 1400°C is uniform with no distinct bright phases observed. Lamellar structure can be obtained in the particles annealed at 1350°C or 1400°C. In addition, the annealed powder shows a porous structure due to the Kirkendall effect, which is conductive to the breakup of coarse particles during the secondary milling.

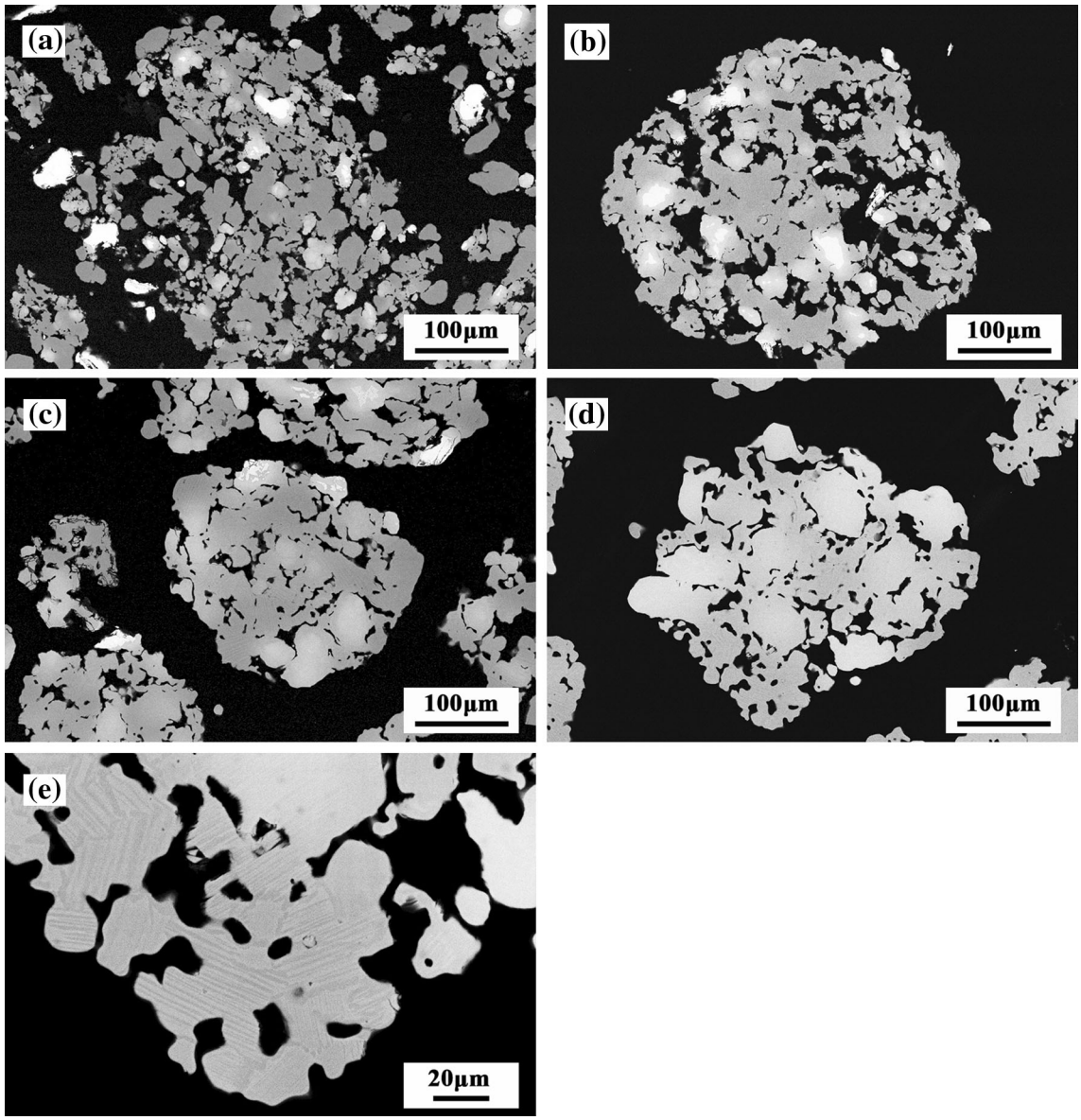

Fig. 3. BSE morphology of powder profiles annealed at different temperatures: (a) 1250°C, (b) 1300°C, (c) 1350°C, and (d and e) 1400°C.

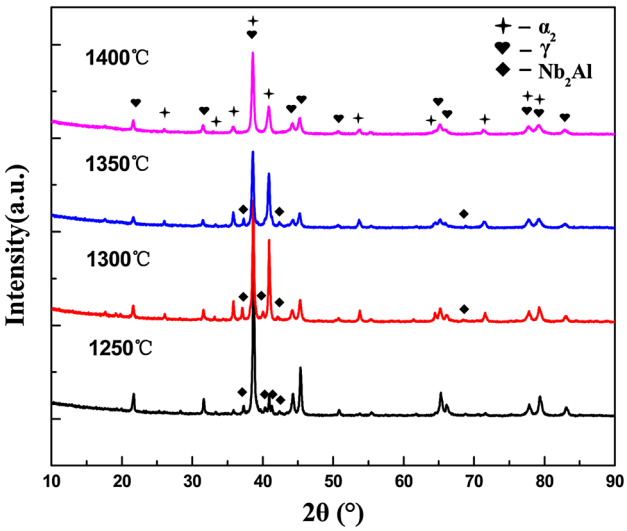

Fig. 4. XRD patterns of the annealed powders.

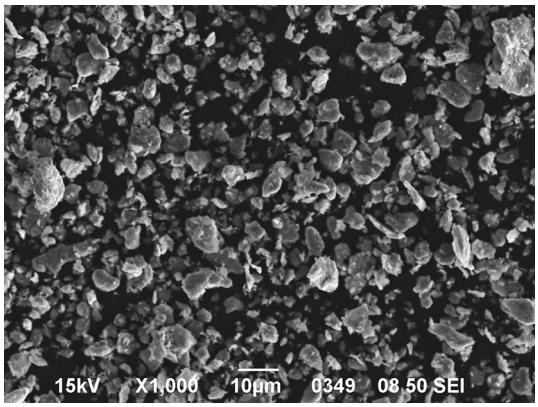

Fig. 5. SEM of the powder after secondary milling.

The XRD patterns of the annealed powders with different temperatures are presented in Fig. 4. The phase constitution varied significantly with annealing temperatures. For the powders treated from 1250°C to 1350°C, remanent σ-Nb_2Al phase corresponding to the bright spots in SEM can be observed, and the amount gradually decreases with the increasing annealing temperature. When annealed at 1400°C, the powder obtained only consists of γ and a small amount of α_2 phase. This is consistent with the SEM analysis. As for the composite structure formed during primary milling, fine Nb and Ti particles are evenly scattered and embedded into Al matrix, leading to the formation of two isolated Nb-Al and Ti-Al systems. For the Ti-Al system, reactions start at a temperature below the melting point of Al and result in γ-TiAl and α_2-Ti_3Al phases during the heating process. For the Nb-Al system, σ-Nb_2Al becomes the final phase with the lowest free energy of formation. With the rise of temperature, Nb_2Al gradually dissolves into the Ti-Al matrix and disappears completely at 1400°C.[30]

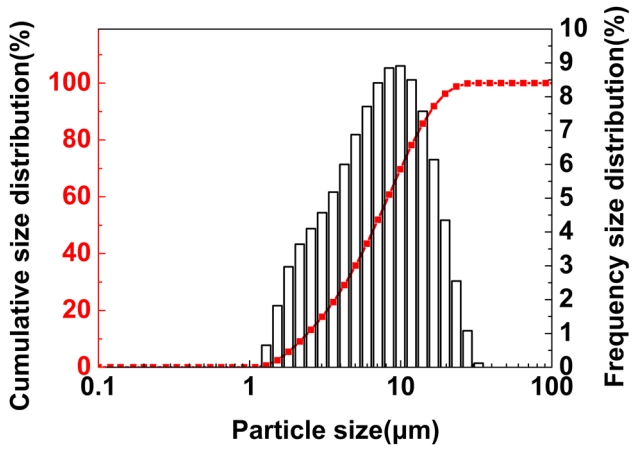

Fig. 6. Particle size distribution of the refined powders.

Besides, during reaction synthesis, the porous structure of the annealed powders formed under the Kirkendall effect due to the difference of the interdiffusion coefficients of Ti and Al atoms.

Figures 5 and 6 portray the surface morphology and particle size distribution of powders obtained after 30 min secondary milling, respectively. SEM observations show that the powders are efficiently refined and most of the particles are smaller than 20 μm in diameter. From Fig. 6, the two-step milled powders exhibit unimodal distribution, and their average particle size, $D(1,0)$, is approximately 8.8 μm.

The impurity contents of the powders are shown in Table I. The alloy powders possess a relatively lower impurity content, although there is a slight increase of oxygen. This is because the abandonment of PCA in primary milling avoids the reactive elemental powders from absorbing C and O from the additive. Moreover, the milling duration is significantly shortened to 4 h and this contributes to the decreased impurity pickup both from the milling balls and the atmosphere. Besides, the primary milled powders, with a larger size and a smaller specific surface, have better oxidation resistance, which reduces the oxidation during annealing and intermediate transit. As for secondary milling, the shortened milling process and passivated prealloyed powder slow down the increase of impurity despite the use of PCA.

Spheroidization Process

The spheroidized powders and their characterization are shown in Figs. 7, 8, and 9. The powders exhibit good sphericity, and almost all powder particles are spherical. The XRD analysis illustrates an obvious change in phase constitution. The spheroidized powder consists of γ and α_2 before spheroidization, whereas α_2 becomes the only remaining phase after spheroidization. This is because, under an extremely high cooling rate in the spheroidization process, some α phase regions have

Table I. Impurity content of the powders (wt.%)

	Powder mixture	Primary milled powder	Annealed powder	Secondary milled powder
C	0.022 (±0.004)	0.029 (±0.002)	0.036 (±0.001)	0.049 (±0.002)
N	0.060 (±0.004)	0.068 (±0.007)	0.063 (±0.002)	0.078 (±0.004)
O	0.24 (±0.02)	0.26 (±0.01)	0.43 (±0.04)	0.48 (±0.02)

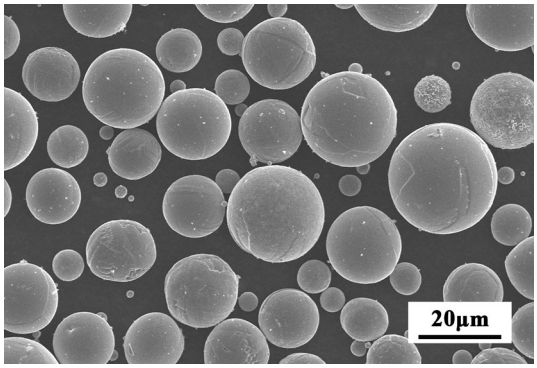

Fig. 7. SEM morphology of the spheroidized powder.

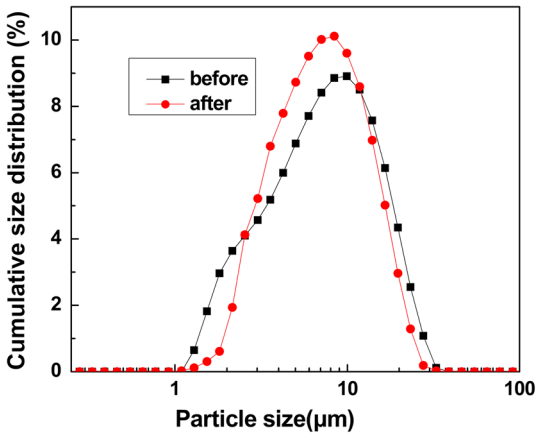

Fig. 8. Particle size distribution comparison of the spheroidized powder.

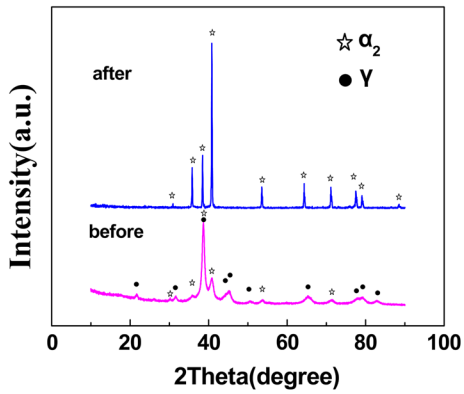

Fig. 9. XRD patterns of the spheroidized powder

no time to precipitate γ phase and they directly transform into the ordering α_2 phase.

The particle size distribution curve reveals a leftward shift after spheroidization. From a geometrical point of view, with the same volume, a sphere has a smaller dimension than any other shapes. This can be regarded to be the main reason. However, it should be pointed out that a reduction in the number of small particles is observed after spheroidization as they are easier to evaporate due to their larger specific surface. As a result, the average particle size of powders shows a little variation after spheroidization, and it is about 8.2 μm.

The oxygen, carbon, and nitrogen contents of the spheroidized powders are 0.47, 0.050, and 0.075%, respectively. The oxygen content shows a slight decrease after spheroidization, which may be attributed to the loss of finer particles.

CONCLUSION

A compact process of two-step ball milling and subsequent RF argon plasma spheroidization from elemental powders has been proposed to fabricate microfine spherical TiAl-Nb alloy powders. The fabrication process and characterization of high-Nb-containing TiAl alloy powders were investigated. It is shown that the alloy powder can be fabricated in quantity by the process based on reaction synthesis and plasma spheroidization. This two-step milling process can be used to prepare uniform alloy powders in a short milling time with no addition of PCA, which makes the process effective and less contaminating. With RF argon plasma processing, the alloy powder can be effectively spheroidized. The powders show good sphericity and compositional homogeneity, and the predominant phase is supersaturated α_2. The powders exhibit an average diameter of about 8.2 μm with a symmetric unimodal particle size distribution. The oxygen and carbon contents of the alloy powders are 0.47% and 0.050%, respectively.

ACKNOWLEDGEMENTS

This research was sponsored by the National Natural Science Foundation of China (No. 51204015) and Aeronautical Science Foundation of China (No. 2013ZE74004).

REFERENCES

1. Y.W. Kim and S.L. Kim, *Intermetallics* 53, 92 (2014).
2. R. Pflumm, et al., *Intermetallics* 53, 45 (2014).

3. S. Shu, et al., *J. Alloys Compd.* 617, 302 (2014).
4. Z.C. Liu, et al., *Intermetallics* 10, 653 (2002).
5. L.L. Xiang, et al., *Intermetallics* 27, 6 (2012).
6. G.E. Bean, M.S. Kesler, and M.V. Manuel, *J. Alloys Compd.* 613, 351 (2014).
7. S. Tian, et al., *Mater. Sci. Eng. A* 614, 338 (2014).
8. L.L. Zhao, et al., *Intermetallics* 18, 1586 (2010).
9. S.H. Khajavi, J. Partanen, and J. Holmström, *Comput. Ind.* 65, 50 (2014).
10. F.P.W. Melchels, et al., *Prog. Polym. Sci.* 37, 1079 (2012).
11. S. Mellor, L. Hao, and D. Zhang, *Int. J. Prod. Econ.* 149, 194 (2014).
12. D.T. Chou, et al., *Acta Biomater.* 9, 8593 (2013).
13. S. Palanivel, et al., *Mater. Des.* 65, 934 (2015).
14. H.P. Shao, et al., *Int. J. Miner. Metall. Mater.* 20, 1076 (2013).
15. H.M. Zhang, et al., *Mater. Sci. Eng. A* 526, 31 (2009).
16. R. Gerling, et al., *Mater. Sci. Eng. A* 252, 239 (1998).
17. G. Wegmann, R. Gerling, and F.P. Schimansky, *Acta Mater.* 51, 741 (2003).
18. M.R. Farhang, A.R. Kamali, and M. Nazarian-Samani, *Mater. Sci. Eng. B* 168, 136 (2010).
19. N. Forouzanmehr, F. Karimzadeh, and M.H. Enayati, *J. Alloys Compd.* 471, 93 (2009).
20. S. Kumaran, et al., *Powder Technol.* 185, 124 (2008).
21. F. Bourg, et al., *Sol. Energy Mater. Sol. Cell* 72, 361 (2002).
22. R. Ye, P. Proulx, and M.I. Boulos, *Int. J. Heat Mass Trans.* 42, 1585 (1999).
23. M.M. Hossain, et al., *Chem. Eng. J.* 150, 561 (2009).
24. Y.W. Sheng, et al., *Proc. Eng.* 36, 299 (2012).
25. S. Kumar, et al., *Mater. Sci. Eng. A* 486, 287 (2008).
26. Z. Károly, J. Szépvölgyi, and Z. Farkas, *Powder Technol.* 110, 169 (2000).
27. V. Chaturvedi, et al., *Ceram. Int.* 40, 8273 (2014).
28. X. Lu, L.P. Zhu, and X.H. Qu, *Key Eng. Mater.* 520, 111 (2012).
29. G. Soucy, et al., *Mater. Sci. Eng. A* 300, 226 (2001).
30. Y.H. Wang, et al., *Trans. Nonferr. Met. Soc.* 16, 853 (2006).